# APE1 upregulates MMP-14 via redox-sensitive ARF6-mediated recycling to promote cell invasion of esophageal adenocarcinoma

**Heng Lu**[1], **Ajaz A. Bhat**[2], **Dunfa Peng**[1], **Zheng Chen**[1,3], **Shoumin Zhu**[1], **Jun Hong**[4], **Selma Maacha**[2], **Jin Yan**[5], **David J. Robbins**[1], **M. Kay Washington**[6], **Abbes Belkhiri**[4], **Wael El-Rifai**[1,3,7]

[1]Department of Surgery, University of Miami Miller School of Medicine, Miami, Florida, USA

[2]Division of Translational Medicine, Research Branch, Sidra Medicine, Doha, Qatar

[3]Department of Veterans Affairs, Miami Healthcare System, Miami, Florida, USA

[4]Department of Surgery, Vanderbilt University Medical Center, Nashville, TN, USA

[5]The First Affiliated Hospital of Nanjing Medical University, Nanjing, Jiangshu, China

[6]Department of Pathology, Vanderbilt University Medical Center, Nashville, TN, USA

[7]Sylvester Comprehensive Cancer Center, University of Miami Miller School of Medicine, Miami, Florida, USA

## Abstract

Esophageal adenocarcinoma (EAC) is an aggressive malignancy with poor clinical outcome. The incidence of EAC has been rising rapidly in the past three decades. Here, we showed that apurinic/apyrimidinic endonuclease (APE1) is overexpressed in EAC cell lines, and patients' samples of dysplasia and EAC. Downregulation of APE1 or inhibition of its redox function significantly repressed invasion. Overexpression of a redox-defective mutant, C65A, abrogated the pro-invasive phenotype of APE1. APE1 regulated invasion via upregulation of matrix metalloproteinase MMP-14 which subsequently activated MMP-2 leading to degradation of the extracellular matrix (ECM) in a redox-dependent manner. Downregulation of APE1 or inhibition of its redox function decreased the rate of endocytosis and recycling of MMP-14 protein. APE1 interacted with ARF6, a key regulator of MMP-14 recycling, which maintained ARF6 activity in an APE1-redox-dependent manner, promoting its ability to regulate MMP-14 recycling to the cell surface. In summary, these findings identify a novel redox-sensitive APE1-ARF6-MMP-14 signaling axis that mediates cellular invasion in esophageal carcinogenesis.

**Keywords**

APE-1/Ref-1; Barrett's; esophageal adenocarcinoma; ARF6; MMP-14; invasion

## Introduction

The incidence of Barrett's esophagus (BE) and esophageal adenocarcinoma (EAC) has increased at an alarming rate over the past few decades in the United States and the Western world (1,2). Chronic gastroesophageal reflux disease (GERD) is the main risk factor for the development of BE and its progression to EAC with invasive and metastatic features (3–6). Previous studies have shown that acidic bile salts (ABS), due to GERD, are implicated in the development of BE and EAC by inducing sustained high levels of oxidative stress, DNA damage, and mitochondrial damage (7–12).

APE1 (apurinic/apyrimidinic endonuclease), also known as redox factor 1 (REF-1), is a dual functional protein. On one hand, APE1 is a key enzyme in DNA base excision repair (BER) pathway, acting as a major apurinic/apyrimidinic endonuclease in the repair of damaged or mismatched nucleotides; on the other hand, APE1 regulates the activity of various redox-dependent transcription factors, such as p53, NF-κB, and STAT3 (13–15) by maintaining critical cysteine residues in a reduced state. The N-terminal Cys65 residue in the APE1 has been identified to mediate the redox function of APE1 (16,17). High expression levels of APE1 have been reported in several cancer types, including EAC, with an associated poor clinical outcome (18). Exposure to acidic bile salts, the main risk factor for EAC, creates a highly oxidative environment with induction and accumulation of APE1 protein in cancer cells (13). APE1 promotes neoplastic cells' survival in this genotoxic environment by mediating repair of oxidative DNA lesions in BE and EAC cells and activating STAT3 pro-survival signaling (13,19). In this context, APE1 induces STAT3 DNA binding and transcriptional activity (13). However, the molecular functions of APE1 in Barrett's tumorigenesis and EAC remain largely understudied.

The matrix metalloproteinase 14 (MMP-14, also known as MT1-MMP) is aberrantly overexpressed in several cancer types (20). MMP-14-activated MMP-2 mediates extracellular matrix (ECM) degradation, a critical step for cancer cells' invasion and metastasis that are associated with poor clinical outcome (21–23). MMP-14 expression and protein levels are regulated by multiple molecular mechanisms (24).

In this study, we report a novel function of APE1 involved in regulating cellular invasion. We demonstrate that APE1 upregulates MMP-14 protein levels via ARF6-mediated endocytosis/recycling. We demonstrate that APE1 interacts with ARF6 and induces ARF6 activity in a redox-dependent manner. Collectively, our findings uncover a novel redox-dependent signaling axis of APE1/ARF6/MMP-14 in promoting invasion of EAC cells.

## Materials and Methods

### Cell lines and reagents

Human CP-B cells were obtained from American Type Culture Collection (ATCC, Manassas, VA, USA). OE19 and ESO26 cell lines were purchased from Sigma-Aldrich (St. Louis, MO, USA). FLO1 and OE33 cell lines were a kind gift from Dr. David Beer (University of Michigan, Ann Arbor, MI, USA). SK-GT-4 cell line was kindly provided from Dr. Xiaochun Xu (MD Anderson, Houston, TX, USA). OE19, OE33 and ESO26 cells were maintained in RPMI medium (GIBCO, Carlsbad, CA, USA), supplemented with 10% fetal bovine serum (FBS) (Invitrogen Life Technologies, Carlsbad, CA, USA), 1% penicillin/streptomycin (GIBCO) and 2mM L-glutamine (GIBCO). FLO-1 and SK-GT-4 cells were maintained in DMEM (GIBCO) containing 10% FBS and 1% penicillin/ streptomycin. CP-B cells were maintained in Keratinocyte-SFM (GIBCO) containing 5% FBS and 1% penicillin/streptomycin. The cells were periodically tested for *mycoplasma* contamination, using mycoplasma detection Kit (PCR) purchased from SouthernBiotech (Birmingham, AL, USA), last checked in December 2018. All cell lines were ascertained to conform to the original *in vitro* morphologic characteristics and were authenticated by using short tandem repeat profiling (Genetica DNA Laboratories, Burlington, NC, USA). All cell lines were used between passages 4 and 15 from the time of their arrivals.

### Antibodies and reagents

Anti-MMP-14 antibody for Western blot was purchased from Abgent (San Diego, CA, USA). Anti-MMP-14 and anti-ARF6 antibodies for immunofluorescence (IF) were purchased from Abcam (Cambridge, MA, USA). Anti-APE1 antibody (MA1–440) and Alexa Fluor™ 488 Phalloidin (A12379) were obtained from Thermo Fisher Scientific (Waltham, MA, USA). Anti-Actin antibody was purchased from Sigma-Aldrich (St. Louis, Missouri, USA). E3330 (APE1 redox-specific inhibitor) was purchased from Novus Biologicals (Littleton, CO, USA), and APE1-i3 (APE1 DNA repair-specific inhibitor) was purchased from MilliporeSigma (Burlington, MA, USA). The usage of inhibitors were following pharmacological studies with recommended doses for the E3330 (25–27) and APE1-i3 (28). Transfection reagents (Polyjet and Lipojet) were obtained from SignaGen Laboratories (Rockville, MD, USA).

### APE1 expression and silencing

A full length of APE1 coding sequence with an N-terminal flag tag was amplified from human cDNA library by PCR using Platinum PCR Supermix High Fidelity (Invitrogen, CA, USA) and was cloned into pcDNA3.1. The APE1 coding sequence from pcDNA3.1-APE1 was subcloned into the Xba I and BamH I restriction sites of adenoviral shuttle vector (PACCMV). APE1 redox-deficient mutant, C65A, and DNA-repair-deficient mutant, H309N, were generated by the QuickChange Lightning Site-Directed Mutagenesis Kit (Agilent Technologies, Santa Clara, CA, USA). Lentivirus particles expressing APE1 shRNA or control shRNA were produced by VectorBuilder Inc (Santa Clara, CA, USA) and then used to transduce CPB, FLO-1, OE33, OE19, and ESO26 cells. To overexpress APE1 and its relevant mutants in APE1-knockdown (shAPE1) cells, the mutation has been introduced into APE1, C65A and H309N expression vectors to avoid APE1-shRNA

targeting, but not change protein sequence. APE1-shRNA targeting sequence is 5'-GCCTGGACTCTCTCATCAATA-3'. Off-target primers' sequences are 5'-AGGAGCTACCAGGTTTATCTCATC-3' and 5'-GATGAGATAAACCTGGTAGCTCCT-3'.

### Cell invasion assays

Cell invasion capability was determined by using a BioCoat™ Matrigel™ Invasion Chamber (Becton-Dickinson, Bedford, MA, USA), following the manufacturer's protocol. Briefly, 20,000 cells suspended in 0.5 ml serum-free medium were seeded into an invasion chamber and 1 ml medium containing 10% serum was seeded onto the lower wells. Chambers were incubated at 37° C for 22 h, after which matrix gel was removed and chambers were fixed and stained with 0.2% (vol/wt) crystal violet. After two washes with PBS, the number of invading cells from at least three fields of each membrane were calculated under light microscope using a 10× objective.

### Immunohistochemistry assay

Tissue microarrays (TMA) containing 61 de-identified archival cases of EACs as well as normal stomach, normal esophagus, and dysplastic and non-dysplastic BE were constructed by Tissue Pathology Core at Vanderbilt University Medical Center, Nashville, TN. All tissue samples were histologically verified and representative regions were selected for inclusion in the TMA. De-waxing and rehydration by descending concentrations of ethanol was followed by antigen retrieval in boiling citrate using a microwave for 10 min. Anti-APE1 antibody (Cell Signaling Technology Danvers, MA), anti-MMP-14 antibody (ab3644, Abcam) and IHC Select® Immunoperoxidase Secondary Detection system (DAB500, MilliporeSigma) were utilized for staining, and specimens were counterstained with hematoxylin, following manufacturer's instructions. Specificity of immunostaining was checked by replacing the primary antibody with non-immune serum. Immunohistochemical results were evaluated for intensity and frequency of the staining and an index score was applied as previously described (29).

### 3D Organotypic culture

3D organotypic cultures of APE1 knockdown cells (shAPE1) and control cells (shCtrl) in CPB or FLO-1 cells were performed, as previously described (30). Briefly, human esophageal fibroblasts (ScienCell, Carlsbad, CA, USA) were seeded into a 3D matrix (75,000 cells/well) containing collagen I (High concentration rat-tail collagen, Corning) and Matrigel (BD Biosciences, Franklin Lakes, NJ, USA) and incubated for 7 days at 37°C. Following incubation, the cells were seeded (500,000 cells/well) on top of the fibroblast matrix. After culturing for an additional 7 days, the cells were harvested, fixed in 70% ethanol and processed for H&E staining and immunocytochemistry.

### Immunocytochemistry of 3D organotypic cell cultures

Paraffin-embedded organotypic culture slides were deparaffinized and rehydrated following standard protocols. Antigen retrieval was performed by boiling the slides in 1M Tris EDTA, pH8.0 for 10 min. Slides were allowed to cool down to room temperature before incubation in 10% normal goat serum blocking solution (Thermo Fisher Scientific) for 30 min. Primary

antibodies of anti-APE1 (diluted at 1:500) and anti-MMP-14 (diluted at 1:200) were added to the slides and incubated overnight at 4°C in a humidified chamber. The next day following incubation, the slides were washed with PBS and incubated with Alexa Fluor conjugated anti-mouse or anti-rabbit secondary antibody (Fluor-488 or Fluor-586) for 1 h at room temperature, protected from light. The slides were washed again with PBS and mounted with a Vectashield mounting medium with DAPI (Vector Laboratories). Images were captured by All-in-One Fluorescence Microscope (BZ-X700, Keyence Corp, Atlanta, GA, USA).

### In-gel zymography

MMP activities were assayed following the manufacturer's instructions (Invitrogen Novex Zymogram Gels, Thermo Fisher Scientific). Briefly, $5 \times 10^5$ cells in a six-well plate were cultured in serum-free medium for 16–24 h, and the conditioned medium was separated on a sodium dodecyl sulfate–polyacrylamide gel electrophoresis gel containing 1 mg/ml gelatin. The gel was washed with buffer I (Tris–HCl [pH 7.5] and 2.5% Triton X-100) incubated overnight in buffer II (150 mM NaCl, 5 mM CaCl$_2$, 50 mM Tris–HCl [pH 7.6]) at 37°C and stained with Coomassie blue. The clear bands indicate where MMPs degraded gelatin.

### *In situ* zymography

Total $10^6$ cells were washed with DMEM and seeded on DQ gelatin fluorescein conjugate (Thermo Fisher Scientific) coated cover glass and cultured with serum-free media for 16 h. The fluorescence release resulting from MMP cleavage of the matrix was visualized by fluorescence microscopy.

### Endocytosis and recycling assays

Cell surface protein biotinylation was performed as previously described (31). The cells were transfected with HA-tagged MMP-14 for overexpression. Sub-confluent cells grown on 60-mm dishes were washed twice with ice-cold PBS and incubated for 15 min. Biotinylation was performed by incubating cells in PBS containing 0.5 mg/ml of the EZ-Link Sulfo-NHS-SS-Biotin (Thermo Fisher Scientific) for 30 min at 4°C, followed by washing and quenching of free biotin. Cells were then incubated at 37°C for different time lapses to allow endocytosis, before two successive reduction reagent (Glutathione) treatments, which can remove the biotin from the cell surface. The cells treated with glutathione without 37°C incubation were used as a negative control, while the cells without glutathione treatment were used as a positive control. To determine endocytic levels of HA-MMP-14 protein, the cells were lysed and the biotinylated surface proteins were precipitated with high capacity streptavidin agarose resin (Thermo Fisher Scientific) and blotted with anti-HA antibody. For recycling assay, the cells were incubated in the first round at 37°C for 10 min to allow endocytosis and treated with a first round of Glutathione. The 2nd round of 37°C incubation at different time lapses allowed recycling and revealed Glutathione stripped all recycled MMP-14. The recycling level can be examined by measuring non-recycled biotin-HA-MMP-14 left on the cell surface (Recycled MMP-14 = Total endocytotic MMP-14 – non-recycled MMP-14).

### Cycloheximide (CHX) chase assay

CPB-scramble and CPB-shAPE1 cells were treated with 100 μg/ml CHX before lysates were collected at different time points and analyzed for MMP-14 protein levels by Western blot analysis. FLO-1 cells were pre-treated with 40μM E3330 for 48 h followed by treatment with CHX. The half-life of MMP-14 protein was determined by relative MMP-14 protein band intensity (MMP-14/actin) at different time points.

### ARF6 activity assay

ARF6 activation assay was performed following the manufacturer's instructions (Cell Biolabs, Inc). Briefly, whole cell lysates from APE1 knockdown cells and scramble shRNA control cells or E3330-treated cells were prepared in RIPA buffer and the active form of ARF6 (GTP-ARF6) was specifically pulled down by GGA3 protein-binding domain (PBD) agarose beads. The effect of APE1 on ARF6 activity was further validated by Western blot analysis. Quantification was based on relative ARF6 protein band intensity (GTP-ARF6/ total ARF6).

### Proximity ligation assay

*In situ* protein-protein interactions were detected using the Duolink *in situ* proximity ligation assay (PLA) detection kit (Sigma-Aldrich) following the manufacturer's instructions. Cells were cultured in 8-well chamber slides for 24 h and then washed in PBS and fixed with 4% paraformaldehyde buffer for 45 min at room temperature. Cells were then permeabilized in 0.5% Triton X-100 in PBS for 5 min, blocked for 45 min at room temperature with gentle shaking, and incubated overnight at 4°C with the two primary antibodies raised against the two proteins of interest, each from a different host species. The primary antibodies (APE1, Mouse monoclonal, Thermo Fisher Scientific; ARF6, Rabbit Monoclonal, Abcam) were used. Hybridizations, ligations, washings, and detection steps were performed following the supplier's protocol. After final washes in buffer B, cells were mounted using the Duolink *in situ* mounting medium with DAPI, sealed with nail polish, and allowed to dry for 15 min at room temperature before imaging using the All-in-One Fluorescence Microscope (BZ-X700, Keyence Corp, Atlanta, GA).

### Statistical analysis

All the results were expressed as mean ± SEM. Differences were analyzed by student's *t*-test or one-way ANOVA followed by the Bonferroni post-hoc test. All statistical analyses were performed using the GraphPad Prism, version 5.0 (GraphPad Software). $p < 0.05$ was considered statistically significant.

## Results

### APE1 silencing decreases cell invasion capabilities

Earlier studies have shown that APE1 is highly expressed in tissue samples and representative cell lines of dysplastic BE and EAC (13,19). To study the functional role of APE1 in EAC, we generated stable APE1-knockdown cell lines (shAPE1) and relevant control knockdown cells (shCtrl) in CPB and FLO-1 cells (Figure1A). Interestingly, we

observed that APE1 knockdown (shAPE1 cells) changed the cellular shape from spindle-like to a cobblestone-like shape (Figure1B). This remarkable morphology change is usually associated with enhanced invasion capabilities. Therefore, we performed *in vitro* matrigel invasion assay to determine the impact of APE1 knockdown on cell invasion. APE1 silencing significantly diminished relative invasion ratio ($p < 0.05$) in CPB and FLO-1 cells, as compared to control cells (Figure1C), consistent with cell morphology changes. Additionally, APE1 knockdown by siRNA confirmed that APE1 is required for FLO-1 cell invasion (Supplementary Figure S1A &B).

## APE1 redox function is required for cell invasion

APE1 is a multi-function protein with DNA base excision repair and redox functions. To determine which function of APE1 is involved in APE1-dependent cell invasion capabilities, we treated CPB, FLO-1, OE19, and ESO26 cells with specific APE1 inhibitors, E3330 or APE1-i3, respectively. E3330, is a known APE1 redox-specific inhibitor, whereas APE1-i3 is mainly an inhibitor of DNA damage repair function of APE1 (28). By using *in vitro* matrigel invasion assays, we found that E3330 treatment significantly diminished cell invasion ($p < 0.01$), whereas APE1-i3 treatment had no significant effect on invasion, as compared to control cells (Figure 2A, and Supplementary Figure S2A). Interestingly, we also observed that E3330 treatment changed FLO-1 cell morphology (spindle-like) to a less invasive shape (cobblestone-like), whereas, APE1-i3 didn't induce these changes (Supplementary Figure S2B). To avoid their cytotoxic effects on cell viability, we treated cells with relatively low doses of these inhibitors on our invasion experiments (Supplementary Figure S2C). To verify the inhibitors' functions, we reconstituted APE1 expression in APE1-knockdown (shAPE1) FLO-1 cells by overexpression of control vector (Ctrl), FLAG-tagged wild-type APE1, APE1-C65A (redox-defective mutant) or APE1-H309N (DNA-repair-defective mutant) (32). APE1 silencing decreased FLO-1 cells invasion, comparing shAPE1 to shCtrl. More importantly, we detected a significant rescue of cell invasion by reconstitution of wild-type APE1 or H309N mutant, as compared to the control vector (Ctrl) ($p < 0.05$). However, unlike wild-type APE1 or H309N mutant, redox-defective C65A mutant failed to rescue cell invasion ($p < 0.01$). The ectopic expression of flag-tagged wild-type APE1 or relevant mutants was confirmed by Western blot analysis (Figure 2B). Additionally, we found that the C65A mutant did not promote cell invasion as wild-type APE1 or H309N mutant in OE33 and SK-GT-4 cells (Supplementary Figure S2D). Taken together, these results indicate that the redox function of APE1, not DNA repair function, is required for cellular invasion.

## APE1 upregulates MMP-14 protein levels in dysplastic BE and EAC

Overexpression of MMP-14 is known to mediate invasion in several cancer types. Western blot analysis suggested a correlation between APE1 and MMP-14 in several esophageal cell lines; CPB, FLO-1, and ESO26 cells showed higher protein levels of APE1 and MMP-14, whereas OE19, OE33, and SK-GT-4 cells exhibited lower levels of both proteins (Figure 3A). Stable APE1-silencing induced a consistent decrease in MMP-14 protein levels in several cell models, including CPB, FLO-1, OE33, OE19, and ESO26 cell lines (Figure 3B). We also observed similar results in transient APE1 knockdown by siRNA in FLO-1 cells (Supplementary Figure S1B). Conversely, overexpression of APE1, by an adenoviral

expression system, in cell models with low endogenous levels consistently increased MMP-14 protein levels in OE33 and SK-GT-4 cells (Figure 3C). Furthermore, we investigated the protein levels of APE1 and MMP-14 in normal esophagus, non-dysplastic BE, dysplastic BE, and EAC tissues by immunohistochemistry (IHC) in tissue microarrays (TMA) (Figure 3D). The results demonstrated similar protein expression profiles of MMP-14 and APE1, as indicated by the lack of expression in normal esophagus tissues, weak expression in non-dysplastic BE, and high expression in dysplastic BE and EAC. A summary of IHC scores is given in Supplementary Table S1. Of note, dysplastic BE and EAC tissue samples demonstrated significantly higher protein levels of MMP-14 ($p < 0.01$) and APE1 ($p < 0.01$) than normal and non-dysplastic BE tissues. In dysplastic BE and EAC tissues, MMP-14 IHC staining was on the cell surface and cytosol, whereas APE1 staining was diffuse nuclear and cytosolic. Pearson's correlation analysis indicated a trend of association between MMP-14 and APE1 in EAC tissues, although not statistically significant ($p = 0.149$), possibly due to small sample size.

### APE1 upregulates MMP-14 protein level on cell surface via its redox function

The cell surface expression of MMP-14 is critical for extracellular matrix (ECM) degradation and cancer cell invasion. We, therefore, performed immunofluorescence staining to examine the role of APE1 on MMP-14 cell surface localization and expression. APE1 silencing significantly decreased MMP-14 protein levels on the cell surface in CPB and FLO-1 cells, as compared to control cells ($p < 0.05$, Figure 4A). Next, we examined the effects of APE1 redox function on MMP-14 cell surface expression. Immunofluorescence data indicated that inhibition of APE1 redox activity by E3330 had no effect on APE1 protein levels or cellular localization, as expected, but significantly diminished MMP-14 on cell surface in CPB and FLO-1 cells, relative to control cells ($p < 0.05$, Figure 4B). Moreover, Western blot analysis (Supplementary Figure S3A) and immunofluorescence staining (Supplementary Figure S3B) showed C65A mutant could not rescue MMP-14 expression as wild-type APE1 or H309N in APE1-knockdown (shAPE1) FLO-1 cells. By using organotypic 3D culture system, we confirmed that APE1-silencing decreased MMP-14 protein levels, as compared to control cells (Figure 4C). Additionally, H&E staining showed APE1 silencing (shAPE1) greatly reduced invasive cells (indicated with red arrows) which breached into the basement membrane and infiltrated into the Matrigel containing fibroblasts layer in the organotypic 3D culture (Supplementary Figure S3C). Collectively, our results suggest that APE1 up-regulates MMP-14 protein on cell surface through APE1-dependent redox function.

### APE1 redox function is required for MMP-14 activity

MMP-14 is known to cleave MMP-2 pro-form (72 kDa) to generate MMP-2 active-form (62 kDa) (33). To investigate whether APE1 and its redox function are required for MMP-14 activity, we examined APE1 effects on MMP-14 activation of MMP-2 proteinase. We concentrated conditioned media (C.M.) to detect total MMP-2, and collected whole cell lysates (WCL) for APE1 and MMP-14 protein analysis. Western blot results indicated that APE1 knockdown decreased protein levels of MMP-2 (pro-form, 72 kDa), as well as MMP-14 in CPB and FLO-1 cells, as compared to the relevant control cells (Figure 5A). Additionally, in-gel zymography assay data revealed that APE1 silencing significantly

decreased active-MMP-2 levels in C.M. in CPB and FLO-1 cells relative to control cells, respectively (p < 0.01, Figure 5B). At the same time, we found that APE1-knockdown had no effect on MMP-9 activation, suggesting that MMP-2, not MMP-9, is the downstream effector of APE1-MMP-14-dependent invasion. Furthermore, *in situ* zymography assay data indicated that APE-1 knockdown or inhibition of APE1-specific redox function by E3330 significantly reduced ECM degradation activities, as demonstrated by levels of quenched fluorescein-labeled gelatin (DQ-gelatin), in CPB and FLO-1 cells, as compared to control cells, respectively ($p < 0.01$, Figure 5C & D).

**APE1 regulates MMP-14 protein stability**

To determine how APE1 regulates MMP-14, we first investigated if APE1 affects MMP-14 mRNA levels. Quantitative real-time PCR (qPCR) data indicated that APE1-silencing had no significant effect on MMP-14 mRNA levels in CPB, FLO-1, or OE33 cells, as compared to control cells, respectively (Supplementary Figure S4A). These results suggested that APE1 regulates MMP-14 through a post-transcriptional mechanism at the protein level. By using cycloheximide (CHX) chase assay to determine possible changes in MMP-14 half-life, we found that APE1 silencing decreased MMP-14 protein half-life from ~4 h to ~1 h in CPB cells (Figure 5E) and from ~11 h to ~4 h in FLO-1 cells (Figure 5F). Additionally, inhibition of APE1 redox activity by E3330 significantly decreased MMP-14 protein half-life from ~10 h to ~4 h in FLO-1 cells as compared to control cells (Supplementary Figure S4B). Taken together, these data indicated that APE1 mediated MMP-14 protein stability, not mRNA expression in a redox-dependent manner.

**APE1 redox function is required for MMP-14 endocytic trafficking**

Endocytosis and recycling are the most critical regulatory processes of cellular MMP-14 protein in cancer invasion. To investigate the role of APE1 in the endocytic trafficking of MMP-14, we monitored endocytosis and recycling of exogenously expressed HA-MMP-14 protein following APE1 knockdown in FLO-1 cells. The internalized HA-MMP-14 protein was detected by Biotin-Streptavidin pull-down at different time points. APE1-knockdown completely abolished MMP-14 endocytosis at 5 min ($p < 0.01$) and dramatically decreased it at 7.5 min ($p < 0.05$), relative to control cells (Figure 6A). At 10 min, we observed a decrease in endocytic MMP-14 in control cells (shCtrl, as compared to 7.5 min time point, suggesting that endocytic MMP-14 has been partially recycled back to the cell surface at 10 min. The results strongly suggested that APE1 silencing significantly slowed down the rate of MMP-14 endocytosis in EAC cells. Moreover, consistent with APE1 knockdown data, inhibition of APE1 redox function by E3330 significantly enhanced endocytic MMP-14 at 5 min ($p < 0.01$) and at 7.5 min ($p < 0.05$) in FLO-1 cells, relative to control cells (Figure 6B). These results suggested that APE1 regulation of the rate of MMP-14 endocytosis involved its redox function. Notably, recycling assay data indicated that APE1-knockdown, as well as APE1 redox function inhibition (E3330), significantly diminished MMP-14 recycling at 7.5 min ($p < 0.05$) and 15 min ($p < 0.01$) in FLO-1 cells, as compared to control cells, respectively (Figure 6C & D). The results indicated that APE1 silencing or inhibition of APE1-redox function significantly delayed MMP-14 recycling. Taken together, our data demonstrated that APE1 and its redox function are required to maintain a high rate of

MMP-14 endocytic trafficking (endocytosis and recycling), a critical factor for cancer invasion.

### APE1 promotes ARF6 activity via interaction and redox function

To further examine the role APE1 has in MMP-14 endocytic trafficking, we screened known major regulators of endocytosis and recycling, such as EHD1, ARF6, Rab5, and Rab4 for protein interaction with APE1 by immunoprecipitation (IP). The results demonstrated a novel protein interaction of ARF6 and APE1, which was strong in FLO-1 cells and consistent in CPB cells (Figure 7A & Supplementary Figure S5A). In line with these results, proximity ligation assay data confirmed the close proximity of ARF6 and APE1 proteins in the cytoplasm in both FLO-1 and CPB cells, as compared to negative control by a single antibody (Figure 7B). As APE1 silencing had no significant effect on ARF6 protein levels in our *in vitro* models (Supplementary Figure S5B), we examined ARF6 activity by GGA3 PBD agarose beads that specifically pull-down GTP-binding ARF6, which is the active form of ARF6. Both stable shRNA knockdown (Figure 7C) and transient siRNA knockdown (Supplementary Figure S5C) of APE1 significantly attenuated ARF6 activities ($p < 0.05$) in CPB and FLO-1 cells relative to control cells, respectively. In addition, APE1 redox inhibition (E3330) significantly decreased active-ARF6 levels ($p < 0.05$) in CPB and FLO-1 cells as compared to control cells, respectively (Figure 7C). However, E3330 treatment or FLAG-tagged APE1-C65A (redox-defective) mutant had no significant effect on APE1-ARF6 interaction (Supplementary Figure S5D & E). Interestingly, ARF6 specific activity inhibitor, NAV-2729 (34), inhibited active ARF6 (GTP-ARF6) and abolished MMP-14 protein elevation induced by APE1-overexpression (Ad-APE1) in OE33 and SK-GT-4 cells (Figure 7D), suggesting that APE1 upregulates MMP-14 in an ARF6-dependent manner. Further, we found NAV-2729 or MMPs inhibitor, GM6001, abolished APE1-elevated invasion capability (p < 0.05) in SK-GT-4 cells (Figure 7E). Collectively, our data revealed a novel redox-sensitive signaling axis of APE1/ARF6/MMP-14 in cancer cell invasion. A cartoon summarizing our data is shown in Figure 7F.

## Discussion

Chronic gastro-esophageal reflux disease is the main risk factor for the development of BE and its progression to EAC. Exposure of esophageal cells to acidic bile salts, the mimicry of GERD episodes, can induce overexpression of APE1 in BE and EAC cells (13,19). In this study, we uncovered a novel function of APE1 in promoting cancer cell invasion and report a molecular signaling axis that includes APE1, ARF6, and MMP-14 in cancer cell invasion.

Our findings suggest that overexpression of APE1 is required to promote invasion abilities in EAC cells. We consistently found that knockdown of APE1 or inhibition of its redox function remarkably diminished invasion. In fact, APE1 is known as a reducing donor and its cysteine 65 (cys65)-redox activity is essential to maintain a reduced status on specific cysteine residues of APE1-associated transcriptional factors and other signaling proteins (13,35). Unlike wild-type APE1 or H309N (DNA-repair-deficient mutant), overexpression of a redox-deficient APE1 mutant (C65A) failed to promote invasion in our models of EAC, confirming that APE1 redox activity is required for APE1 pro-invasion function. The role of

APE1 in promoting cell migration or invasion has been described in other cancer types such as breast cancer cells (36), pancreatic cancer cells (37) and hepatocellular carcinoma cell lines (38). However, the mechanism by which APE1 mediates invasion, remains unclear and largely unknown.

To our knowledge, our study is the first to describe the role of APE1 in promoting cell invasion in EAC or Barrett's tumorigenesis. Therefore, we initiated investigations of the underlying mechanism by which APE1 mediates cell invasion. It is widely known that the persistent high levels of MMP-14 on cell surface enhances MMP-2 activation (39,40) and ECM degradation (21–23), facilitating cancer cell migration and invasion (24,41–43). Here we present several lines of evidence indicating that APE1 is required for increasing MMP-14 and active MMP-2, and ECM degradation. IHC staining of tissue array indicated a possible positive correlation between MMP-14 and APE1 protein levels in dysplastic BE and EAC. Indeed, we demonstrated that APE1 silencing or blockade of APE1 redox function decreased MMP-14 protein levels, MMP-2 activity and ECM degradation. The results confirm that APE1 regulates MMP-14/MMP-2/ECM degradation signaling cascade. Among ECM components, multiple targets of MMP-14 and MMP-2 cleavage activities include CD44 (44), Notch1 (45), VEGF (46) and latent TGF-ß (47), suggesting that APE1-redox/ MMP-14/MMP-2 axis could activate multiple signaling pathways associated with cancer cell invasion.

Although APE1 is recognized as a transcriptional co-factor for its redox regulation on important transcriptional factors, such as p53, NF-κB and STAT3 (13–15), our study clearly indicated that APE1 elevated MMP-14 protein levels on cell surface by modulating endocytosis and recycling, not through mRNA regulation. Our results demonstrate a different signaling axis for APE1, not reported in earlier invasion studies (38). Furthermore, proximity ligation and immunoprecipitation assays revealed a close proximity and an interaction between APE1 and ARF6 proteins. Notably, the main cellular functions of ARF6 include regulation of endocytosis and recycling of plasma membrane proteins (48,49). ARF6 plays a critical role in regulating MMP-14 endocytic trafficking, required for maintaining high protein levels of MMP-14 on cancer cell surface that mediates ECM degradation/ remodeling and invasion (50–52). We demonstrated that APE1 redox function is critical for ARF6 activity and ARF6-mediated MMP-14 endocytic trafficking. Genetic knockdown or redox-specific inhibition (E3330) of APE1 repressed ARF6 activity and consequently decelerated MMP-14 endocytosis/recycling, suggesting that overexpression of APE1 activates ARF6 through its redox-function in cancer cells. We also observed clear effects of APE1 and redox on MMP-14 protein stability, which may be due to repressed recycling, increasing the chance of uptake of MMP-14 by lysosome for degradation. In addition, ARF6 activity inhibitor, NAV-2729, abrogated APE1-induced MMP-14 protein accumulation, further confirming the APE1 – ARF6 axis in upregulating MMP-14 recycling and protein levels. We also observed decreased pro-MMP-2 (72kDa) protein in the conditioned media from APE1-knockdown cells. It is possible that APE1-redox/ARF6 signaling axis can regulate the endocytic trafficking of other cancer-associated cell surface proteins or secretory proteins, such as MMP-2.

While most patients undergoing radiofrequency ablation (RFA) for dysplastic BE achieve eradication of intestinal metaplasia, 25% or more develop recurrence of BE (53). Identifying the precise etiology and molecular mechanisms for the recurrence of Barrett's metaplasia after RFA remains a challenging clinical problem. A recent study suggested that the presence of sub-squamous intestinal metaplasia (SSIM) may be the driving factor in some patients. SSIM is defined as the presence of intestinal-type metaplastic glands underneath esophageal squamous epithelium (54,55). Development of SSIM involves the invasion of Barrett's epithelial cells into the lamina propria of adjacent squamous epithelium (54,55). We previously reported that ABS treatment, mimicking GERD conditions in patient's esophagus, induced APE1 protein levels in non-neoplastic BE and EAC cells (13,19). Combined with our findings in this study, this raises the possibility that the oxidative environment induced by GERD may promote cell invasion in BE and EAC tumorigenesis through APE1-redox/ARF6/MMP-14 signaling axis. In this context, the development of APE1 inhibitors may be useful in both non-neoplastic and neoplastic settings of BE and EAC. However, further studies are needed to verify the role of APE1 in SSIM and BE recurrence in patients.

In summary, our study identified a novel signaling axis for APE1 in promoting cancer cell invasion by activating ARF6-mediated MMP-14 recycling via APE1-redox function. This signaling axis may be critical in promoting invasion and progression not only in Barrett's tumorigenesis and EAC, but possibly in other cancer types.

## Supplementary Material

Refer to Web version on PubMed Central for supplementary material.

## Acknowledgements

## REFERENCES

1. Jemal A, Siegel R, Xu J, Ward E. Cancer statistics, 2010. CA Cancer J Clin 2010;60:277–300 [PubMed: 20610543]

2. Kong CY, Kroep S, Curtius K, Hazelton WD, Jeon J, Meza R, et al. Exploring the recent trend in esophageal adenocarcinoma incidence and mortality using comparative simulation modeling. Cancer Epidemiol Biomarkers Prev 2014;23:997–1006 [PubMed: 24692500]

3. Sital RR, Kusters JG, De Rooij FW, Kuipers EJ, Siersema PD. Bile acids and Barrett's oesophagus: a sine qua non or coincidence? Scand J Gastroenterol Suppl 2006;11–7 [PubMed: 16782617]

4. Bernstein H, Bernstein C, Payne CM, Dvorak K. Bile acids as endogenous etiologic agents in gastrointestinal cancer. World J Gastroenterol 2009;15:3329–40 [PubMed: 19610133]

5. Lagergren J Adenocarcinoma of oesophagus: what exactly is the size of the problem and who is at risk? Gut 2005;54 Suppl 1:i1–5 [PubMed: 15711002]

6. Reid BJ, Li X, Galipeau PC, Vaughan TL. Barrett's oesophagus and oesophageal adenocarcinoma: time for a new synthesis. Nat Rev Cancer 2010;10:87–101 [PubMed: 20094044]

7. Nehra D, Howell P, Williams CP, Pye JK, Beynon J. Toxic bile acids in gastro-oesophageal reflux disease: influence of gastric acidity. Gut 1999;44:598–602 [PubMed: 10205192]

8. Bernstein H, Payne CM, Bernstein C, Schneider J, Beard SE, Crowley CL. Activation of the promoters of genes associated with DNA damage, oxidative stress, ER stress and protein malfolding by the bile salt, deoxycholate. Toxicol Lett 1999;108:37–46 [PubMed: 10472808]

9. Sokol RJ, Winklhofer-Roob BM, Devereaux MW, McKim JM Jr. Generation of hydroperoxides in isolated rat hepatocytes and hepatic mitochondria exposed to hydrophobic bile acids. Gastroenterology 1995;109:1249–56 [PubMed: 7557092]

10. Peng DF, Hu TL, Soutto M, Belkhiri A, El-Rifai W. Glutathione Peroxidase 7 Suppresses Bile Salt-Induced Expression of Pro-Inflammatory Cytokines in Barrett's Carcinogenesis. J Cancer 2014;5:510–7 [PubMed: 24963355]

11. Inayama M, Hashimoto N, Tokoro T, Shiozaki H. Involvement of oxidative stress in experimentally induced reflux esophagitis and esophageal cancer. Hepatogastroenterology 2007;54:761–5 [PubMed: 17591057]

12. Jenkins GJ, Cronin J, Alhamdani A, Rawat N, D'Souza F, Thomas T, et al. The bile acid deoxycholic acid has a non-linear dose response for DNA damage and possibly NF-kappaB activation in oesophageal cells, with a mechanism of action involving ROS. Mutagenesis 2008;23:399–405 [PubMed: 18515815]

13. Bhat AA, Lu H, Soutto M, Capobianco A, Rai P, Zaika A, et al. Exposure of Barrett's and esophageal adenocarcinoma cells to bile acids activates EGFR-STAT3 signaling axis via induction of APE1. Oncogene 2018

14. Fishel ML, Kelley MR. The DNA base excision repair protein Ape1/Ref-1 as a therapeutic and chemopreventive target. Mol Aspects Med 2007;28:375–95 [PubMed: 17560642]

15. Tell G, Quadrifoglio F, Tiribelli C, Kelley MR. The many functions of APE1/Ref-1: not only a DNA repair enzyme. Antioxid Redox Signal 2009;11:601–20 [PubMed: 18976116]

16. Walker LJ, Robson CN, Black E, Gillespie D, Hickson ID. Identification of residues in the human DNA repair enzyme HAP1 (Ref-1) that are essential for redox regulation of Jun DNA binding. Mol Cell Biol 1993;13:5370–6 [PubMed: 8355688]

17. Tell G, Fantini D, Quadrifoglio F. Understanding different functions of mammalian AP endonuclease (APE1) as a promising tool for cancer treatment. Cell Mol Life Sci 2010;67:3589–608 [PubMed: 20706766]

18. Yuan CL, He F, Ye JZ, Wu HN, Zhang JY, Liu ZH, et al. APE1 overexpression is associated with poor survival in patients with solid tumors: a meta-analysis. Oncotarget 2017;8:59720–8 [PubMed: 28938675]

19. Hong J, Chen Z, Peng D, Zaika A, Revetta F, Washington MK, et al. APE1-mediated DNA damage repair provides survival advantage for esophageal adenocarcinoma cells in response to acidic bile salts. Oncotarget 2016;7:16688–702 [PubMed: 26934647]

20. Lafleur MA, Xu D, Hemler ME. Tetraspanin proteins regulate membrane type-1 matrix metalloproteinase-dependent pericellular proteolysis. Mol Biol Cell 2009;20:2030–40 [PubMed: 19211836]

21. Lee S, Jilani SM, Nikolova GV, Carpizo D, Iruela-Arispe ML. Processing of VEGF-A by matrix metalloproteinases regulates bioavailability and vascular patterning in tumors. J Cell Biol 2005;169:681–91 [PubMed: 15911882]

22. Rundhaug JE. Matrix metalloproteinases and angiogenesis. Journal of cellular and molecular medicine 2005;9:267–85 [PubMed: 15963249]

23. Carmeliet P Mechanisms of angiogenesis and arteriogenesis. Nature medicine 2000;6:389–95

24. Castro-Castro A, Marchesin V, Monteiro P, Lodillinsky C, Rosse C, Chavrier P. Cellular and Molecular Mechanisms of MT1-MMP-Dependent Cancer Cell Invasion. Annu Rev Cell Dev Biol 2016;32:555–76 [PubMed: 27501444]

25. Kelley MR, Luo M, Reed A, Su D, Delaplane S, Borch RF, et al. Functional analysis of novel analogues of E3330 that block the redox signaling activity of the multifunctional AP endonuclease/redox signaling enzyme APE1/Ref-1. Antioxid Redox Signal 2011;14:1387–401 [PubMed: 20874257]

26. Ding J, Fishel ML, Reed AM, McAdams E, Czader MB, Cardoso AA, et al. Ref-1/APE1 as a Transcriptional Regulator and Novel Therapeutic Target in Pediatric T-cell Leukemia. Mol Cancer Ther 2017;16:1401–11 [PubMed: 28446640]

27. Fehrenbacher JC, Guo C, Kelley MR, Vasko MR. DNA damage mediates changes in neuronal sensitivity induced by the inflammatory mediators, MCP-1 and LPS, and can be reversed by enhancing the DNA repair function of APE1. Neuroscience 2017;366:23–35 [PubMed: 28965839]

28. Rai G, Vyjayanti VN, Dorjsuren D, Simeonov A, Jadhav A, Wilson DM 3rd, et al. Synthesis, biological evaluation, and structure-activity relationships of a novel class of apurinic/apyrimidinic endonuclease 1 inhibitors. J Med Chem 2012;55:3101–12 [PubMed: 22455312]

29. Peng DF, Razvi M, Chen H, Washington K, Roessner A, Schneider-Stock R, et al. DNA hypermethylation regulates the expression of members of the Mu-class glutathione S-transferases and glutathione peroxidases in Barrett's adenocarcinoma. Gut 2009;58:5–15 [PubMed: 18664505]

30. Le Bras GF, Loomans HA, Taylor CJ, Revetta FL, Andl CD. Activin A balance regulates epithelial invasiveness and tumorigenesis. Lab Invest 2014;94:1134–46 [PubMed: 25068654]

31. Wu X, Gan B, Yoo Y, Guan JL. FAK-mediated src phosphorylation of endophilin A2 inhibits endocytosis of MT1-MMP and promotes ECM degradation. Dev Cell 2005;9:185–96 [PubMed: 16054026]

32. Maher RL, Bloom LB. Pre-steady-state kinetic characterization of the AP endonuclease activity of human AP endonuclease 1. J Biol Chem 2007;282:30577–85 [PubMed: 17724035]

33. Ingvarsen S, Madsen DH, Hillig T, Lund LR, Holmbeck K, Behrendt N, et al. Dimerization of endogenous MT1-MMP is a regulatory step in the activation of the 72-kDa gelatinase MMP-2 on fibroblasts and fibrosarcoma cells. Biol Chem 2008;389:943–53 [PubMed: 18627313]

34. Yoo JH, Shi DS, Grossmann AH, Sorensen LK, Tong Z, Mleynek TM, et al. ARF6 Is an Actionable Node that Orchestrates Oncogenic GNAQ Signaling in Uveal Melanoma. Cancer Cell 2016;29:889–904 [PubMed: 27265506]

35. Vascotto C, Bisetto E, Li M, Zeef LA, D'Ambrosio C, Domenis R, et al. Knock-in reconstitution studies reveal an unexpected role of Cys-65 in regulating APE1/Ref-1 subcellular trafficking and function. Mol Biol Cell 2011;22:3887–901 [PubMed: 21865600]

36. Guerreiro PS, Corvacho E, Costa JG, Saraiva N, Fernandes AS, Castro M, et al. The APE1 redox inhibitor E3330 reduces collective cell migration of human breast cancer cells and decreases chemoinvasion and colony formation when combined with docetaxel. Chem Biol Drug Des 2017;90:561–71 [PubMed: 28303665]

37. Zou GM, Maitra A. Small-molecule inhibitor of the AP endonuclease 1/REF-1 E3330 inhibits pancreatic cancer cell growth and migration. Mol Cancer Ther 2008;7:2012–21 [PubMed: 18645011]

38. Zheng ZH, Du W, Li YJ, Gao MQ, Huang AM, Liu JF. Lentiviral-mediated short hairpin RNA silencing of APE1 suppresses hepatocellular carcinoma proliferation and migration: A potential therapeutic target for hepatoma treatment. Oncol Rep 2015;34:95–102 [PubMed: 25976295]

39. Itoh Y, Takamura A, Ito N, Maru Y, Sato H, Suenaga N, et al. Homophilic complex formation of MT1-MMP facilitates proMMP-2 activation on the cell surface and promotes tumor cell invasion. EMBO J 2001;20:4782–93 [PubMed: 11532942]

40. Stanton H, Gavrilovic J, Atkinson SJ, d'Ortho MP, Yamada KM, Zardi L, et al. The activation of ProMMP-2 (gelatinase A) by HT1080 fibrosarcoma cells is promoted by culture on a fibronectin substrate and is concomitant with an increase in processing of MT1-MMP (MMP-14) to a 45 kDa form. J Cell Sci 1998;111 (Pt 18):2789–98 [PubMed: 9718371]

41. Shiomi T, Okada Y. MT1-MMP and MMP-7 in invasion and metastasis of human cancers. Cancer Metastasis Rev 2003;22:145–52 [PubMed: 12784993]

42. Poincloux R, Lizarraga F, Chavrier P. Matrix invasion by tumour cells: a focus on MT1-MMP trafficking to invadopodia. J Cell Sci 2009;122:3015–24 [PubMed: 19692588]

43. Friedl P, Alexander S. Cancer invasion and the microenvironment: plasticity and reciprocity. Cell 2011;147:992–1009 [PubMed: 22118458]

44. Marrero-Diaz R, Bravo-Cordero JJ, Megias D, Garcia MA, Bartolome RA, Teixido J, et al. Polarized MT1-MMP-CD44 interaction and CD44 cleavage during cell retraction reveal an essential role for MT1-MMP in CD44-mediated invasion. Cell Motil Cytoskeleton 2009;66:48–61 [PubMed: 19023892]

45. Ma J, Tang X, Wong P, Jacobs B, Borden EC, Bedogni B. Noncanonical activation of Notch1 protein by membrane type 1 matrix metalloproteinase (MT1-MMP) controls melanoma cell proliferation. J Biol Chem 2014;289:8442–9 [PubMed: 24492617]

46. Dean RA, Butler GS, Hamma-Kourbali Y, Delbe J, Brigstock DR, Courty J, et al. Identification of candidate angiogenic inhibitors processed by matrix metalloproteinase 2 (MMP-2) in cell-based proteomic screens: disruption of vascular endothelial growth factor (VEGF)/heparin affin regulatory peptide (pleiotrophin) and VEGF/Connective tissue growth factor angiogenic inhibitory complexes by MMP-2 proteolysis. Mol Cell Biol 2007;27:8454–65 [PubMed: 17908800]

47. Sounni NE, Paye A, Host L, Noel A. MT-MMPS as Regulators of Vessel Stability Associated with Angiogenesis. Front Pharmacol 2011;2:111 [PubMed: 21687519]

48. D'Souza-Schorey C, Li G, Colombo MI, Stahl PD. A regulatory role for ARF6 in receptor-mediated endocytosis. Science 1995;267:1175–8 [PubMed: 7855600]

49. Schweitzer JK, Sedgwick AE, D'Souza-Schorey C. ARF6-mediated endocytic recycling impacts cell movement, cell division and lipid homeostasis. Semin Cell Dev Biol 2011;22:39–47 [PubMed: 20837153]

50. Marchesin V, Castro-Castro A, Lodillinsky C, Castagnino A, Cyrta J, Bonsang-Kitzis H, et al. ARF6-JIP3/4 regulate endosomal tubules for MT1-MMP exocytosis in cancer invasion. J Cell Biol 2015;211:339–58 [PubMed: 26504170]

51. Waheed S, Dorjbal B, Hamilton CA, Maxwell GL, Rodriguez GC, Syed V. Progesterone and calcitriol reduce invasive potential of endometrial cancer cells by targeting ARF6, NEDD9 and MT1-MMP. Oncotarget 2017;8:113583–97 [PubMed: 29371931]

52. Loskutov YV, Kozyulina PY, Kozyreva VK, Ice RJ, Jones BC, Roston TJ, et al. NEDD9/Arf6-dependent endocytic trafficking of matrix metalloproteinase 14: a novel mechanism for blocking mesenchymal cell invasion and metastasis of breast cancer. Oncogene 2015;34:3662–75 [PubMed: 25241893]

53. Cotton CC, Haidry R, Thrift AP, Lovat L, Shaheen NJ. Development of Evidence-Based Surveillance Intervals After Radiofrequency Ablation of Barrett's Esophagus. Gastroenterology 2018;155:316–26 e6 [PubMed: 29655833]

54. Anders M, Lucks Y, El-Masry MA, Quaas A, Rosch T, Schachschal G, et al. Subsquamous extension of intestinal metaplasia is detected in 98% of cases of neoplastic Barrett's esophagus. Clin Gastroenterol Hepatol 2014;12:405–10 [PubMed: 23891922]

55. Zhang Q, Agoston AT, Pham TH, Zhang W, Zhang X, Huo X, et al. Acidic Bile Salts Induce Epithelial to Mesenchymal Transition via VEGF Signaling in Non-Neoplastic Barrett's Cells. Gastroenterology 2018

## Significance:

This study demonstrates the association between oxidative stress and the development and metastatic behavior of esophageal adenocarcinoma
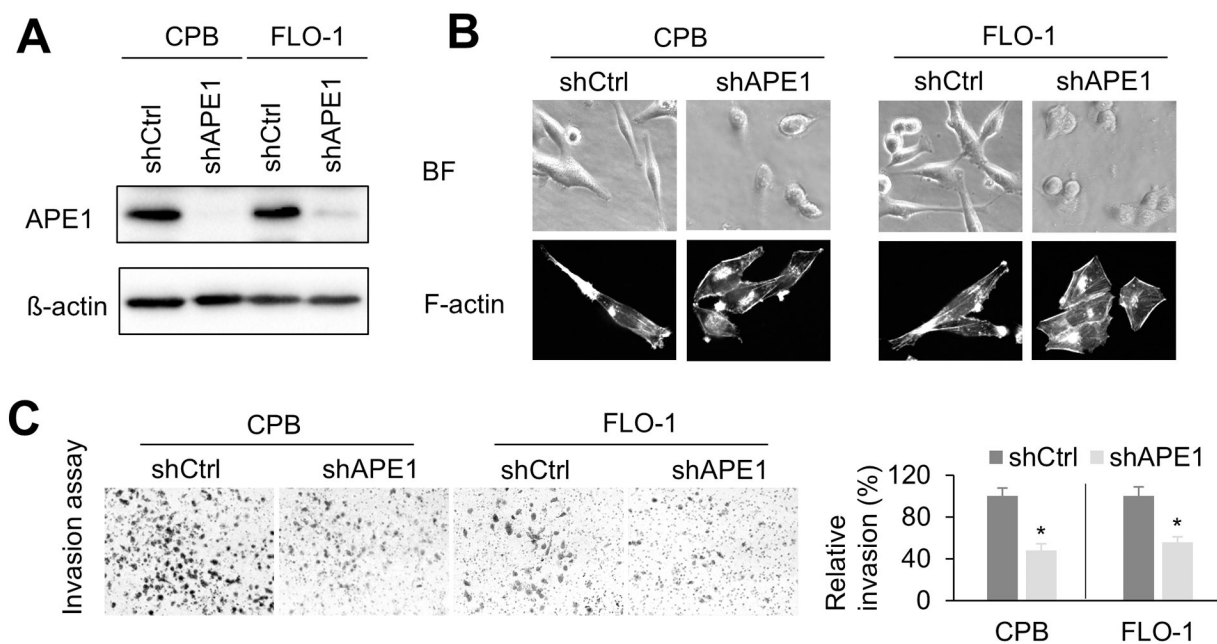
**Figure1. silencing decreases invasion capacity.**

**A**, Western blot analysis of CPB and FLO-1 cells with APE1-knockdown (shAPE1) or control (shCtrl). **B**, Representative cell images of bright field (BF) and F-actin staining in APE1-knockdown cells or control cells. Alexa Fluor™ 488 Phalloidin was used for F-actin staining. **C**, invasion assays were performed using APE1-knockdown cells or respective control cells. The results were expressed as the mean ± SEM of three independent experiments. *, $p < 0.05$.
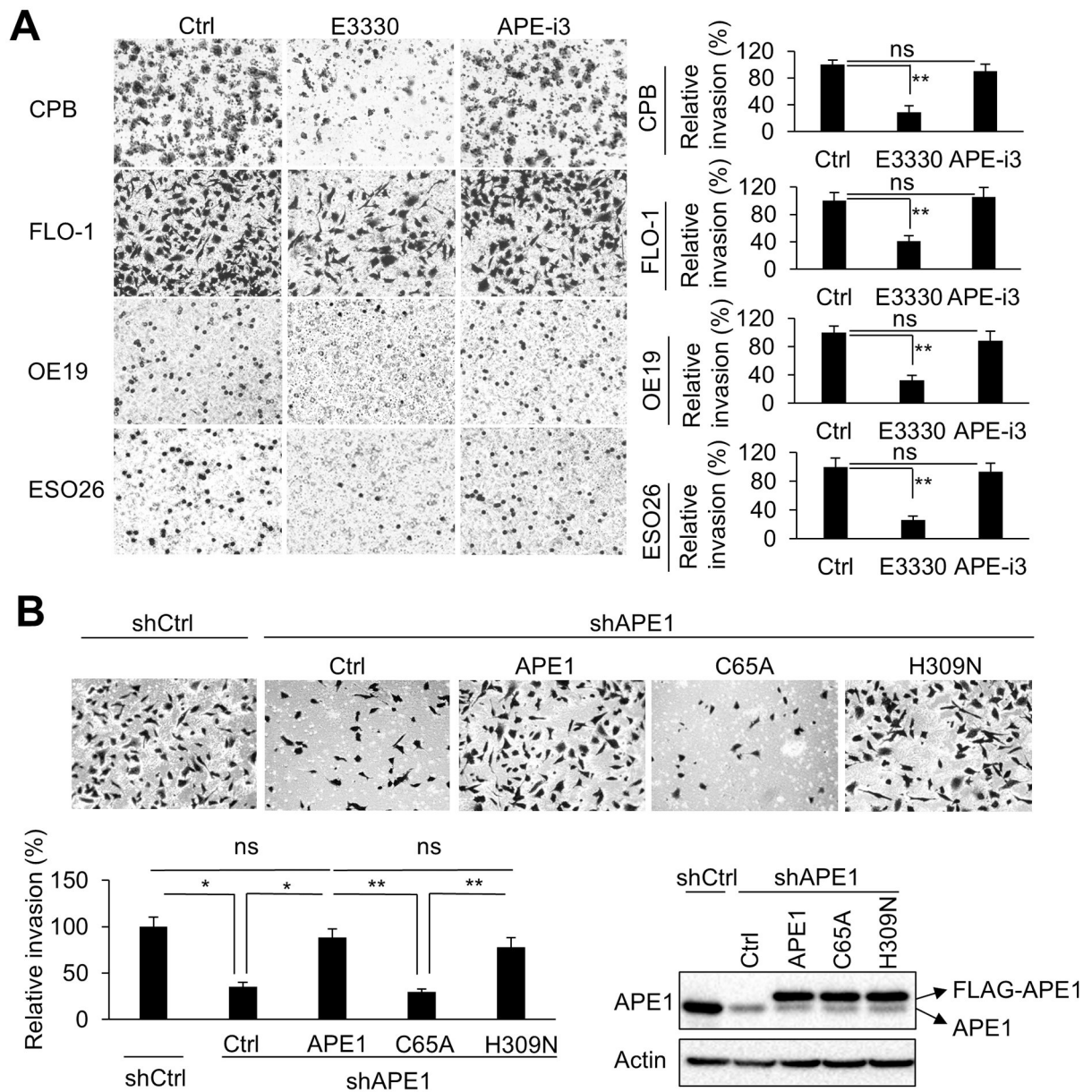
**Figure 2. Redox function of APE1 is required for invasion.**
**A**, Representative images (magnification: 200x) of the invasion assays. CPB, FLO-1, OE19, and ESO26 cells were pre-treated overnight with 40μM E3330 (APE1 redox function inhibitor), 0.5μM APE1-iIII (APE1 DNA repair function inhibitor), or vehicle control (Ctrl), followed by collecting cells for invasion assays. The inhibitors were maintained in the invasion chambers and bottom wells during the assays. **B**, Representative images (magnification: 200x) of the invasion assays in FLO-1 cells. Control vector (Ctrl), FLAG-tagged wild-type APE1, C65A (redox defective mutant) or H309N (DNA repair defective mutant) was overexpressed in APE1-knockdown (shAPE1) FLO-1 cells. The mutation to avoid APE1-shRNA targeting has been generated in those overexpression vectors. Scramble shRNA was used as control (shCtrl). Endogenous APE1, overexpression of FLAG-tagged
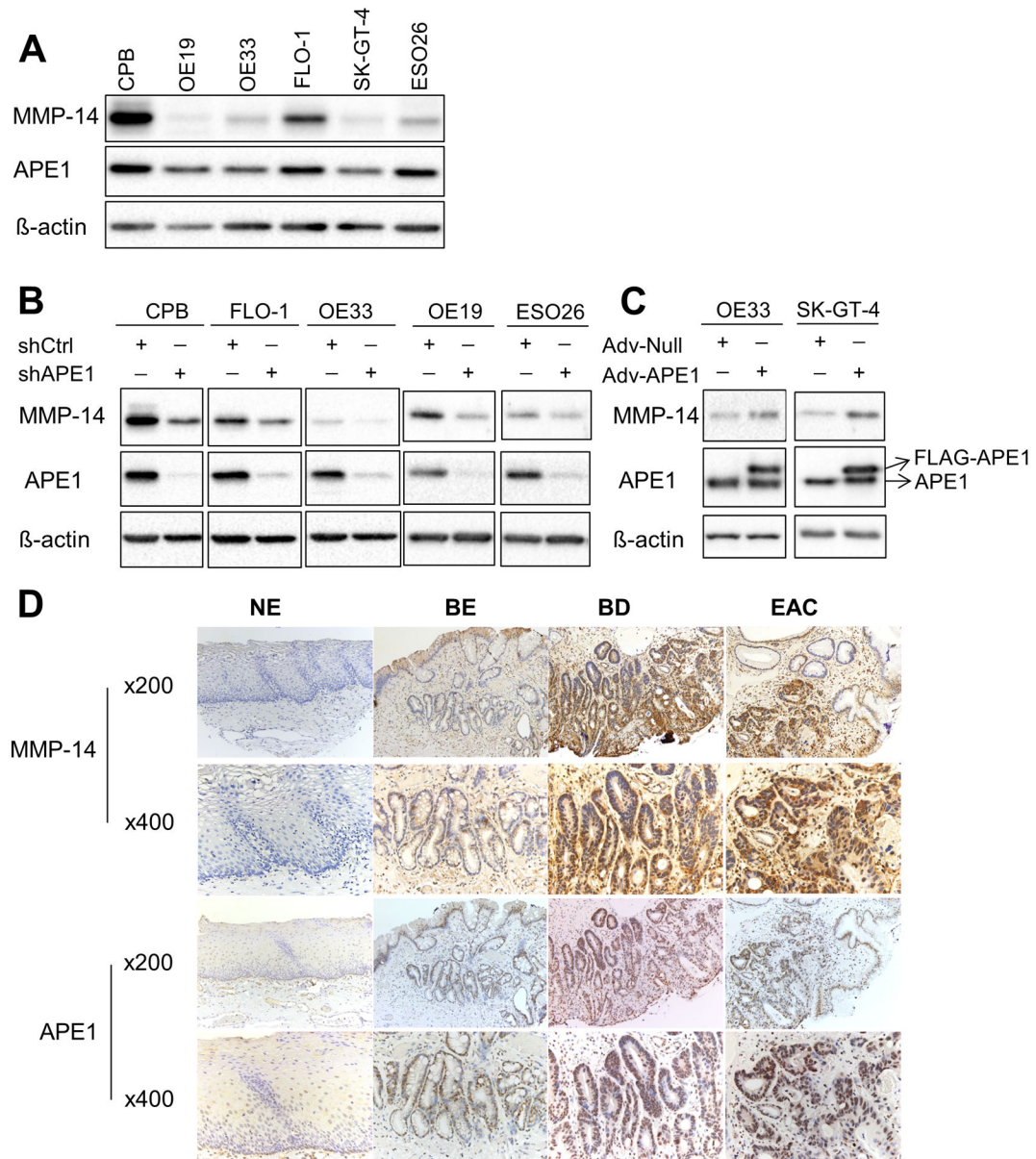
APE1 and its relevant mutants were examined by Western blot analysis. All quantification analyses were based on independent triplicate experiments. *, $p < 0.05$; **, $p < 0.01$; ns, no significance.
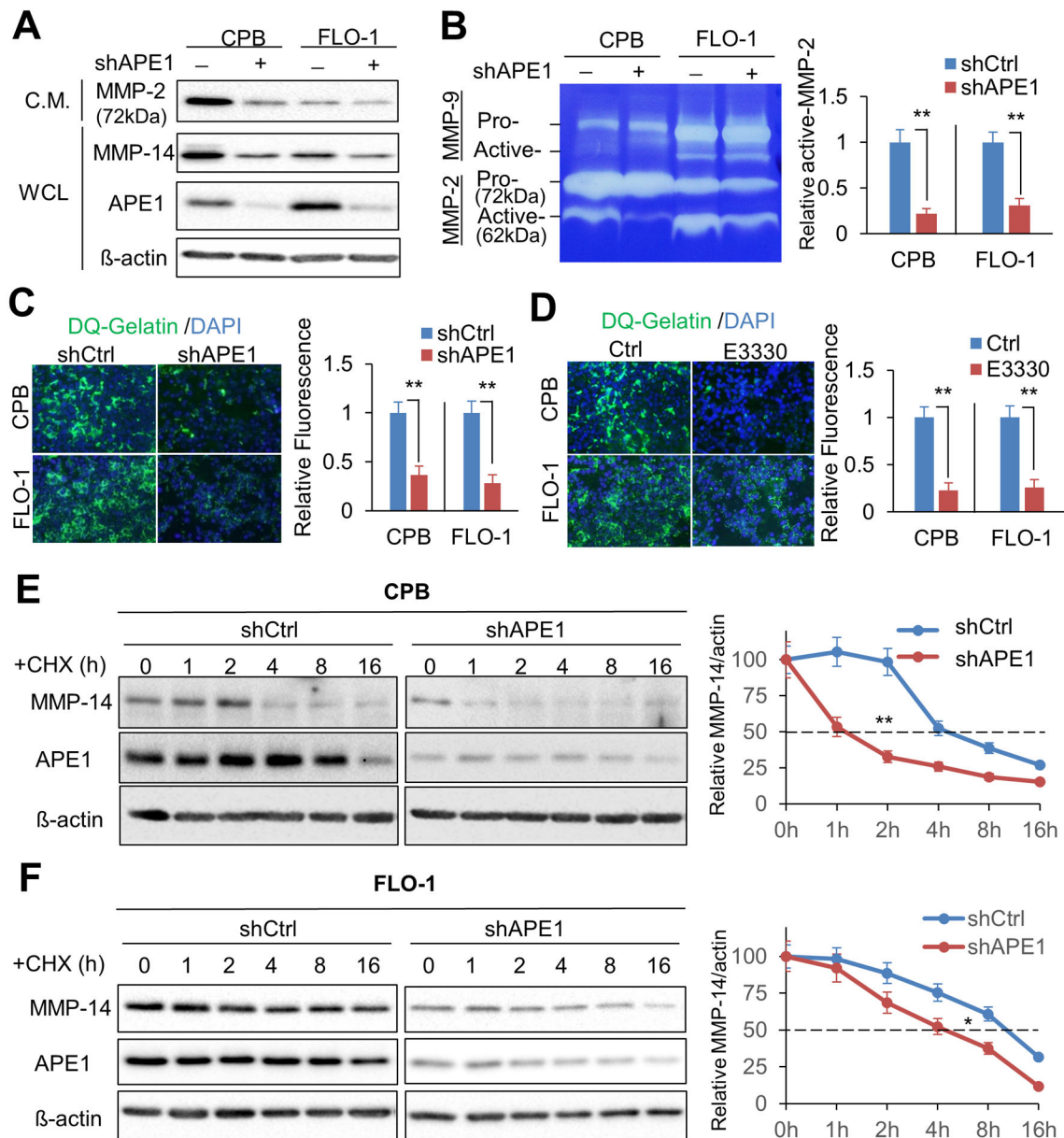
**Figure 3. MMP-14 protein level is regulated by APE1 in BE and EAC cell lines.**
**A**, Western blot analysis of APE1 and MMP-14 protein profiles in dysplastic Barrett's cell line (CPB) and EAC cell lines. **B**, MMP-14, APE1 and ß-actin protein levels were examined by Western blot analysis in CPB, FLO-1, OE33, OE19 and ESO26 cells with stable APE1 knockdown (shAPE1). Stable scramble shRNA (shCtrl) was used as the control. **C**, APE1 was overexpressed in OE33 and SK-GT-4 cells by using adenoviral infection particles (Adv-APE1). Adv-Null was used as the control. The protein samples were collected 72 h post infection for Western blot analysis of MMP-14, APE1, and ß-actin. **D**, Representative immunohistochemistry staining images of MMP-14 and APE1 in normal esophagus (NE), non-dysplastic Barrett's esophagus (BE), dysplastic Barrett's esophagus (BD) and esophageal adenocarcinoma (EAC).
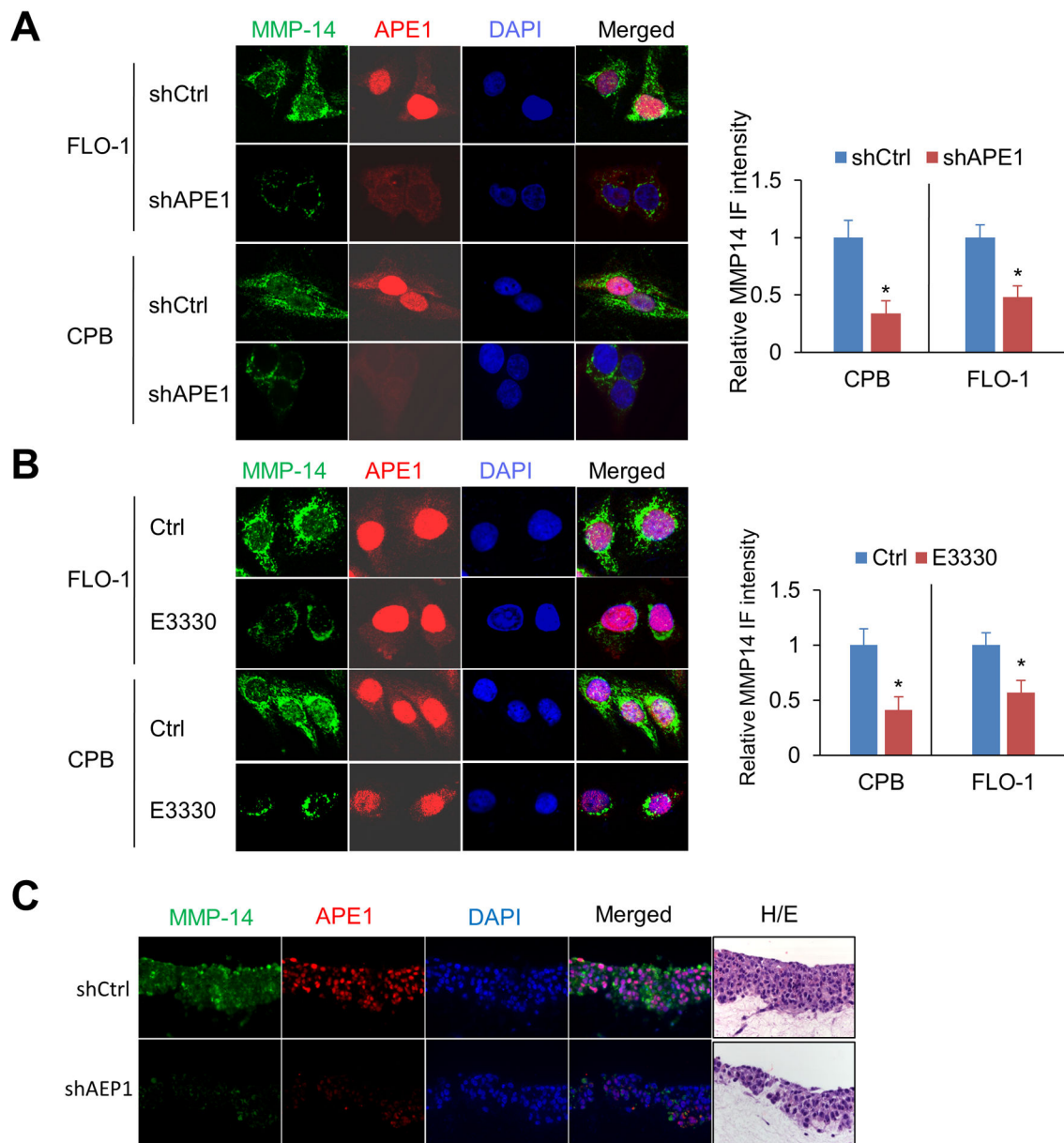
**Figure 4. APE1 silencing or APE1 redox-specific inhibition decreases MMP-14 protein levels.**
Representative immunofluorescent images of MMP-14 (green) and APE1 (red) in FLO-1 or
CPB cells; nuclei were stained with DAPI (blue). **A**, APE1 stable knockdown cells
(shAPE1), and their control cells (shCtrl). **B**, Cells were treated with 40μM E3330 or vehicle
control (Ctrl) for 24 h before staining. **C**, 3D organotypic culture of CPB cells with stable
knockdown (shAPE1) or control (shCtrl). Hematoxylin and eosin (H&E) staining of
sequential cut of the same blocks used for immunofluorescence staining. The quantification
of MMP-14 intensity was expressed as the mean ± SEM of 3 independent fields. *, $p < 0.05$.

**Figure 5. Knockdown of APE1 reduces active MMP-2 form and ECM degradation by down-regulating MMP-14 protein level.**

**A**, Conditioned medium (C.M.) from CPB, FLO-1 or relevant APE1 knockdown cells were collected, concentrated, and examined by Western blot analysis for MMP-2. The whole cell lysates from the relevant dishes were collected for Western blots to detect MMP-14, APE1 and ß-actin. **B**, In-gel zymography assay. The concentrated conditioned medium was loaded in gelatin gel to test MMP-2 activities. Arrows indicate pro- or active- forms of MMPs. Active MMP-2 levels were measured by the intensity ratio of active MMP-2 / actin. **C**, *In situ* zymography assay was performed by using APE1 knockdown cells or control cells on DQ-gelatin pre-coated slides at 48 h post cell seeding. Relative active MMP-2 activities were measured by the active MMP-2/ß-actin. **D**, *In situ* zymography assay by the cells treated with 40μM E3330 or vehicle control (Ctrl). ECM degradation activities were

measured by immunofluorescent intensities. **E & F**, Cycloheximide (CHX) chase assays were performed by using 100μg/ml cycloheximide in CPB (**E**) and FLO-1 (**F**) cells. The cell lysates were collected at the indicated time points for Western blot analysis of APE1 knockdown cells (shAPE1) or control cells (shCtrl). Measurement of MMP-14 protein stability was based on the intensity ratio of MMP-14/actin. All quantification analyses were based on independent triplicate experiments. *, $p < 0.05$; **, $p < 0.01$.
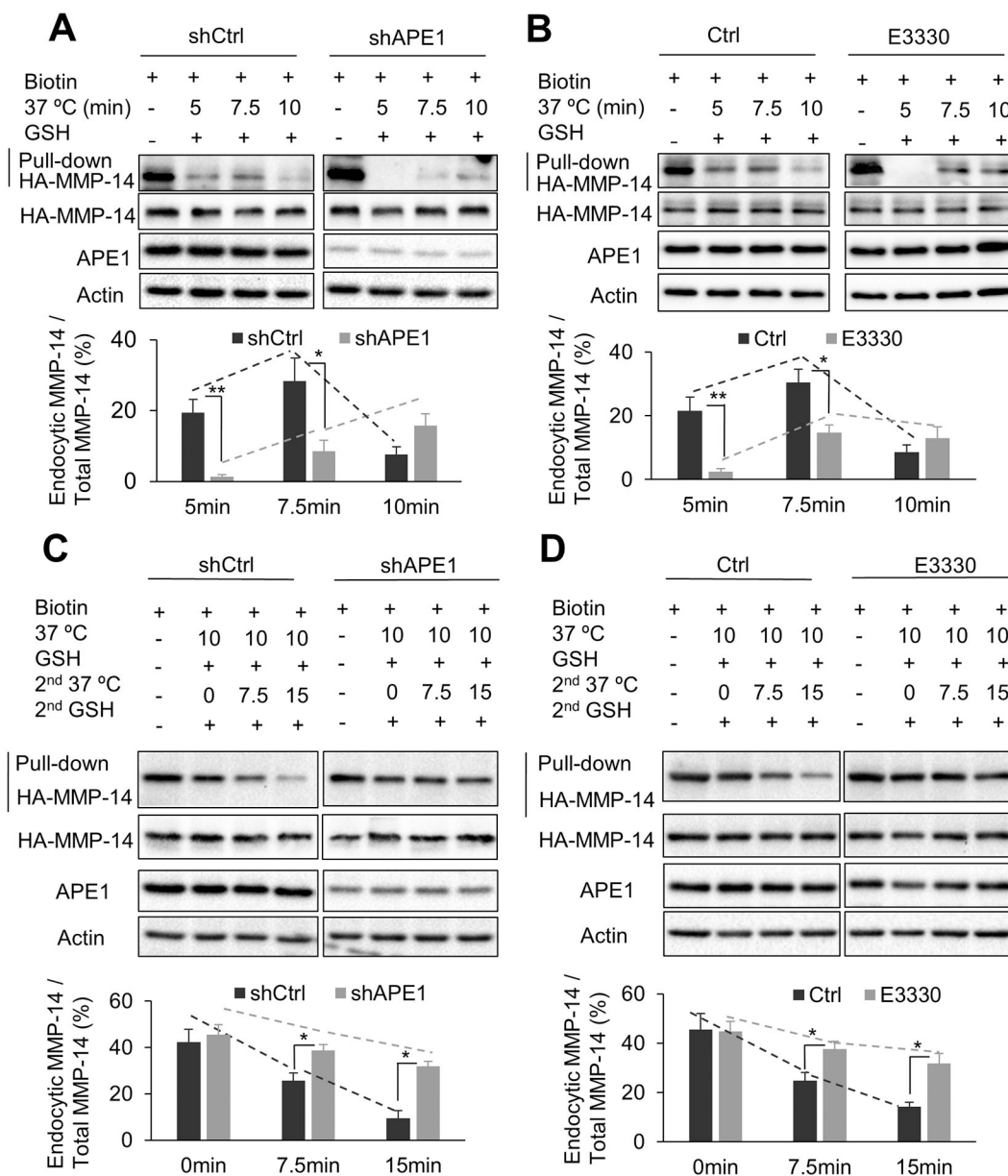
**Figure 6. APE1 is required for the rapid MMP-14 endocytic recycling in EAC cells.**
**A & B**, Endocytosis assays of HA-tagged MMP-14 in FLO-1 cells. Cells were transfected with HA-tagged MMP-14. The cell lysates were collected for biotin pulldown at the indicated time points of endocytosis (37°C incubation). **C & D**, Recycling assays of HA-tag labelled MMP-14 in FLO-1 cells. Recycling assays were performed after 10 min endocytosis (37°C incubation). The cell lysates were collected for biotin pulldown at indicated time courses of recycling (2nd 37°C incubation). APE1-knockdown cells (shAPE1) and control cells (shCtrl) of FLO-1 were used (**A**, **C**). FLO-1 cells were pretreated with 40μM E3330 for 24 h before experiments (**B**, **D**). Relative endocytic MMP-14 levels were measured by the ratio of endocytic MMP-14/total MMP-14. All quantification analyses were based on independent triplicate experiments. *, $p < 0.05$; **, $p < 0.01$.
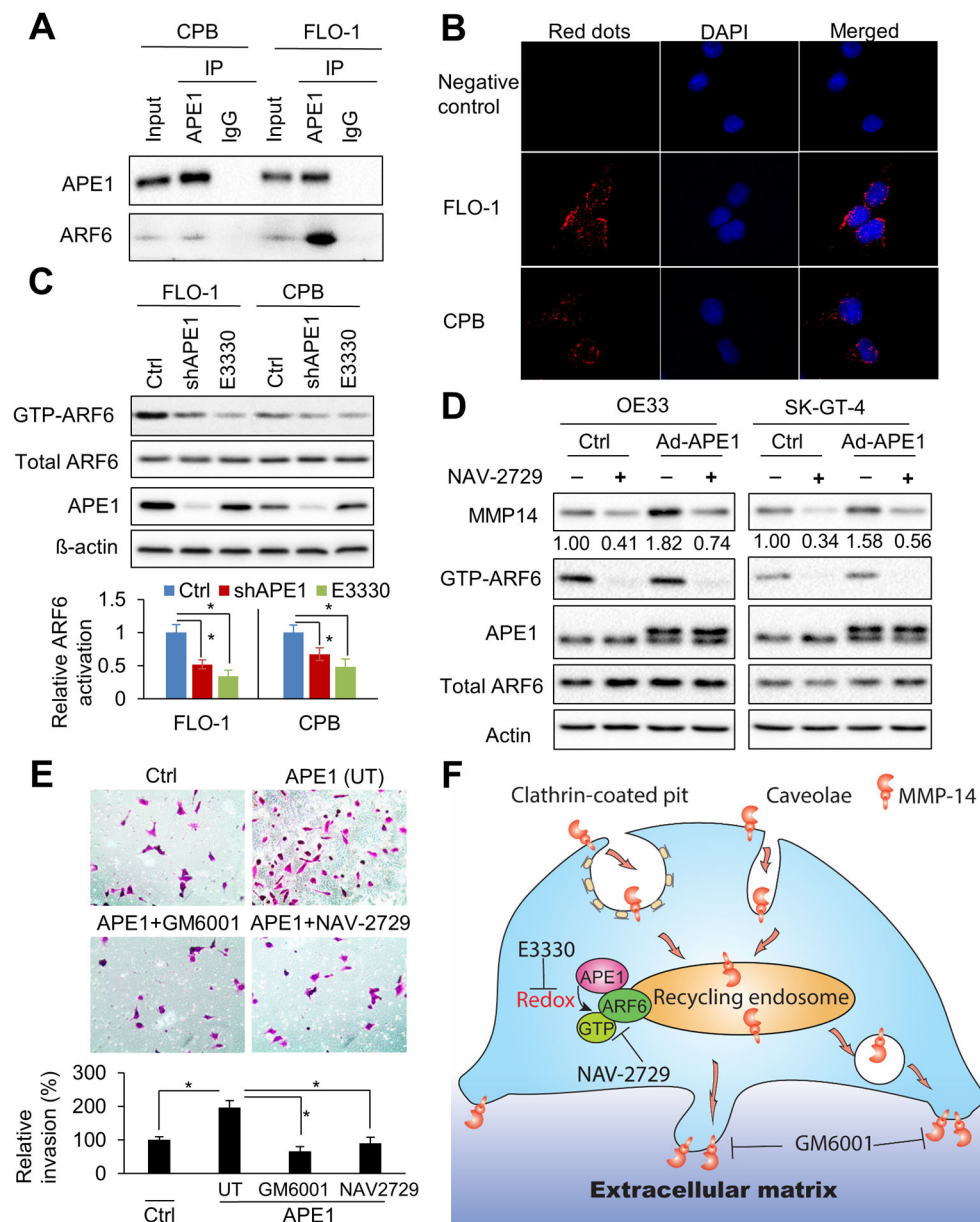
**Figure 7. APE1 promotes ARF6 activity through interaction and redox function.**
**A**, immunoprecipitation (IP) of APE1 in CPB and FLO-1 cells. IgG immunoprecipitation works as a negative control. Western blots of APE1 and ARF6 were performed. **B**, Proximity ligation assays (PLA) in FLO-1 and CPB cells were performed by using anti-ARF6 and anti-APE1 antibodies. Single antibody (anti-ARF6) was used as negative control. **C**, ARF6 activity assays in CPB and FLO-1 cells. The active ARF6 form, GTP-ARF6, was specifically pulled down from whole cell lysates by GGA3 PBD agarose beads. APE1, total ARF6, and ß-actin in whole cell lysates, and GTP-ARF6 in pulldown products were examined by Western blots. Stable APE1-knockdown cells (shAPE1), control cells (Ctrl) or the cells with 24 h pretreatment of 40μM E3330 were harvested for cell lysates. Relative ARF6 activation was measured by the ratio of (GTP-ARF6)/total ARF6. **D**, APE1 was

overexpressed in OE33 and SK-GT-4 cells by adenoviral infection (Ad-APE1). Cells were treated with 1μM specific ARF6 inhibitor, NAV-2729, for 48 h. Whole cell lysates were collected for GTP-ARF6 pulldown and Western blot analysis. **E**, Representative images (magnification: 200x) of the invasion assays in SK-GT-4 cells. Control vector (Ctrl), or wild-type APE1 was overexpressed in the cells. APE1-overexpressed cells were pre-treated and maintained with 10μM MMPs inhibitor, GM6001, or 1uM NAV-2729 through invasion assay. UT, untreated. All quantification analyses were based on independent triplicate experiments. *, $p < 0.05$. **F**, schematic summary of APE1-mediated MMP-14 endocytosis and recycling. MMP-14 is efficiently internalized from plasma membrane by clathrin-dependent or caveolar endocytosis. Active endocytosis and recycling of MMP-14 is critical for extracellular matrix (ECM) degradation and cell invasion. APE1 promotes ARF6 activation through interaction and APE1-redox function. Active ARF6 (GTP-ARF6) in recycling endosome drives quick recycling of MMP-14. APE1 redox inhibitor, E3330, or ARF6 specific inhibitor, NAV-2729, can significantly decrease MMP-14 recycling to cell surface and subsequent cell invasion. Moreover, MMPs inhibitor, GM6001 can inhibit MMP-14 and MMP-2 activities and repress cell invasion.